Electronic structure of $Cu_{100-x}Zr_x$ ($x = 40, 50, 60$) metallic glasses

Weiming Yang [a,b], Haishun Liu [a,*], Qianqian Wang [c], Zhining Wei [a], Lin Xue [b,c], Chaochao Dun [d], Yucheng Zhao [a], Chuntao Chang [b], Baolong Shen [c]

[a] State Key Laboratory for Geomechanics and Deep Underground Engineering, School of Mechanics and Civil Engineering, School of Sciences, China University of Mining and Technology, Xuzhou 221116, People's Republic of China
[b] Key Laboratory of Magnetic Materials and Devices, Ningbo Institute of Materials Technology & Engineering, Chinese Academy of Sciences, Ningbo 315201, People's Republic of China
[c] School of Materials Science and Engineering, Southeast University, Nanjing 211189, People's Republic of China
[d] Department of Physics, Wake Forest University, Winston Salem, NC 27109, USA

ARTICLE INFO

ABSTRACT

The electronic structure of $Cu_{100-x}Zr_x$ ($x = 40, 50, 60$) metallic glasses was investigated by ultraviolet photoelectron spectroscopy and X-ray photoemission spectroscopy, the valence band spectra of these alloys were analyzed by a large shift of the Cu d-band peaks to higher binding energies upon increasing Cu content. Photoemission experiments and first-principles calculations prove that the values of density of states at Fermi level of $Cu_{100-x}Zr_x$ metallic glasses are mainly dominated by Zr rather than Cu. This work will enlighten further research on understanding the inheritance of metallic glasses and designing new metallic glasses with unique properties.

© 2015 Elsevier Ltd. All rights reserved.

1. Introduction

As important systems in condensed matter physics and material science, metallic glasses (MGs) have attracted a great deal of attention over the recent decades [1,2], especially on their structural [3], mechanical [4,5], electrical [6], magnetic [7–9] and superconductive [10] properties. Despite the accumulation of enormous amount of achievement, controlling microalloying and optimizing the design of metallic glass alloys have not been actually realized [11,12]. Recently, Ma et al. [13] revealed that a variety of MGs inherit their elastic modulus from their solvent components. Li et al. [14] proposed that the polyamorphism in densely packed MGs comes from its lanthanide-solvent constituent. Wang [15] revealed that the elastic, plastic and mechanical properties of certain component exhibit some inheritance impacts on the corresponding alloy. However, for some systems, such as Cu-, Pd- and Co-based MGs, their elastic moduli are markedly different from those of the base components [15]. Significant changes in strength, thermal stability, glass-forming ability, corrosion resistance, magnetic properties, and plasticity can be induced by adding minor non-based component to MGs [16–18]. The above inconsistency indicates that the physical understanding of inheritance in metallic glasses is still incomplete. From the electronic theory of solid physics [19], the basic properties of most metal materials are mainly determined by the electrons near the Fermi surface. Therefore, the study of electronic structure would be significant for understanding the inheritance in MGs.

In an attempt to identify the key factors that control the inheritance of MGs, here we study electronic structure of $Cu_{100-x}Zr_x$ ($x = 40, 50, 60$) MGs by combining the ultraviolet photoemission spectroscopy (UPS), X-ray photoemission spectroscopy (xPS) and first-principles calculations. Our results demonstrate that the density of states (DOS) at the Fermi level E_F of Cu–Zr MGs are mainly determined by Zr, which will enlighten further research on designing new MGs with desirable properties.

2. Materials and method

The $Cu_{100-x}Zr_x$ ($x = 40, 50, 60$) MGs with nominal composition were prepared by arc-melting a mixture of pure Cu (99.99%) and Zr (99.99%) in a highly purified argon atmosphere. Glassy ribbons were produced by a rapid quenching technology on a single copper wheel with a speed of 35 m/s. The nature of glassy sample was ascertained by X-ray diffraction (XRD, Bruker D8 Advance) with Cu Kα radiation and differential scanning calorimeter (DSC, NETZSCH 404C) with a heating rate of 0.67 K/s. The bonding states were evaluated by X-ray photoelectron spectroscopy (XPS, Kratos AXIS ULTRA[DLD] instrument) with a monochromic Al Kα X-ray source (hv = 1486.6 eV). The power was 120 W and the X-ray spot size was set to be 700 × 300 μm. The pass energy of the XPS analyzer was set at 20 eV. The base pressure of the analysis chamber

* Corresponding author.
   E-mail address: liuhaishun@126.com (H. Liu).

was lower than 5×10^{-9} Torr. All spectra were calibrated using the binding energy (BE) of C 1s (284.8 eV) as a reference, UV source (He II 40.8 eV) and etching condition (beam energy 2 kV, extract current 100 μA, raster size 4 mm). For the pure components, we use polycrystalline foils of Cu and Zr, which were cleaned by Ar-ion sputtering. We also obtained oxygen-free surfaces of glasses by Ar-ion sputtering.

Calculations have been performed using the first principles simulation package with Vanderbilt ultrasoft pseudopotential, an GGA-PBE exchange–correlation functional, and a plane wave basis with an energy cutoff of 500 eV [20]. Geometry optimization was performed with the Brillouin zone sampling limited to the gamma point, while the Monkhorst–Pack grid with $6 \times 6 \times 6$ k points was used to obtain the accurate density of the electronic states. The electronic self-consistent loop is 5.0×10^{-6} eV, and effort was made to relax model structures until the total forces on each ion were converged to 0.01 eV/Å.

3. Results and discussion

Fig. 1 shows the XRD and DSC traces of $Cu_{100-x}Zr_x$ ($x = 40, 50, 60$) samples. The glass transition temperature (T_g) decreases from 710 K for $x = 40$ to 625 K for $x = 60$, and the crystallization temperature (T_x) decreases from 774 K for $x = 40$ to 682 K for $x = 60$. The XRD patterns of the as-quenched samples display broad diffraction maxima, which is characteristic of an amorphous structure. With increasing Zr content, the broad diffusive amorphous halo peak obviously shifts to a lower wave vector. This can be explained by the incorporation of the larger Zr atoms (atomic radius of 155 pm [21]) replacing the smaller copper atoms (atomic radius of 128 pm [21]), resulting in structural changes of these glasses.

Figs. 2 and 3 show the UPS and XPS spectra of the $Cu_{100-x}Zr_x$ ($x = 40, 50, 60$) MGs, respectively. For comparison, polycrystalline Cu and Zr were measured under the same experimental settings. The spectra without background subtraction has been done and the energy distribution DOS are given. There are some differences between the spectra measured with UPS and XPS, indicating the existence of the final-state effects and the significant change of matrix elements over the energy of the valence band. Both Figs. 2 and 3 show that the Zr spectrum has two main peaks: the one located just below the Fermi level is due to the weakly filled 4d band, with a width around 3.8 eV, and the other peak is more like a shoulder at higher binding energy. The DOS of $Cu_{100-x}Zr_x$ ($x = 40, 50, 60$) metallic glasses in the vicinity of the Fermi level

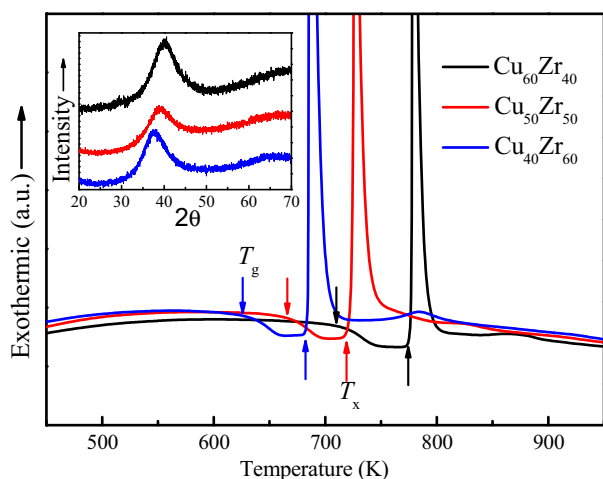**Fig. 2.** UPS spectra of $Cu_{100-x}Zr_x$ ($x = 40, 50, 60$) MGs, polycrystalline Cu and Zr.

Fig. 3. XPS spectra of $Cu_{100-x}Zr_x$ ($x = 40, 50, 60$) MGs, polycrystalline Cu and Zr.

mainly come from Cu 3d states and Zr 4d states. As shown in Fig. 3, upon increasing Cu content in the alloys, the high-binding-energy in position on alloying Cu remain constant, whereas the low-binding-energy edges are shifted considerably by about 0.8 eV in Cu–Zr glasses. The center of Zr 4d band of MGs is slightly shifted to lower binding energy, whereas the Cu 3d band shift is about 1 eV to higher binding energy. The DOS of the $Cu_{100-x}Zr_x$ ($x = 40, 50, 60$) MGs in the vicinity of the Fermi level is slightly reduced compared to pure Zr. In these systems, the Cu states are localized and the Zr states are relatively delocalized [22]. Therefore, the delocalized DOS at the Fermi level E_F of MGs are thought to be determined mainly by Zr 4d states.

To further gain insights into the electronic structure of $Cu_{100-x}Zr_x$ MGs, the DOS of crystalline CuZr of B2 structure was calculated using first principles computations and is shown in Fig. 4. This simplification is justified by the similarity of local structure and electronic properties between MGs and their crystalline counterparts revealed by photoemission measurements [23,24]. As we can see from Fig. 4, the total DOS of ordered compound Cu_1Zr_1 is constituted by 4s, 4p and 3d states of Cu and 5s, 5p and 4d states of Zr. However, the DOS at Fermi level E_F is mainly dominated by Zr 4d states. In order to compare the DOS of the glassy $Cu_{50}Zr_{50}$ and its crystalline counterpart Cu_1Zr_1, the XPS spectra of $Cu_{50}Zr_{50}$ glass were normalized in such a way that the ratio of the areas

Fig. 1. DSC curves for as-quenched $Cu_{100-x}Zr_x$ ($x = 40, 50, 60$) alloys; the inset shows the XRD traces of the samples in as-quenched state.
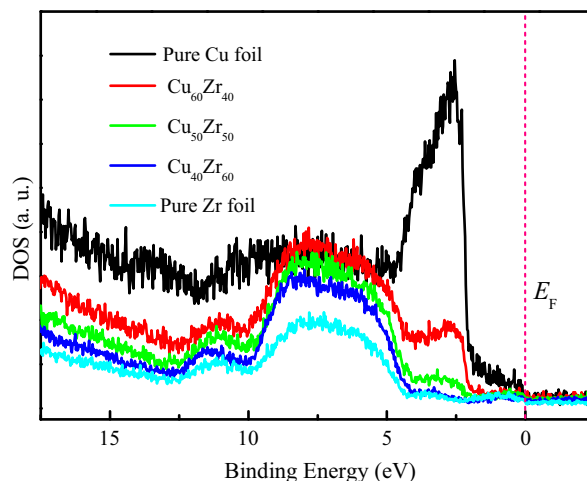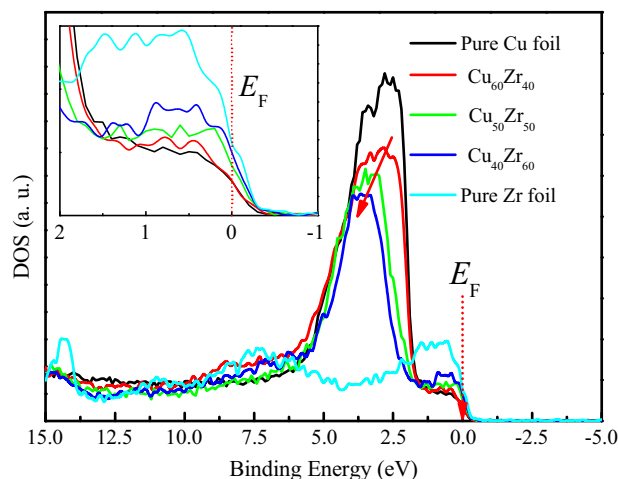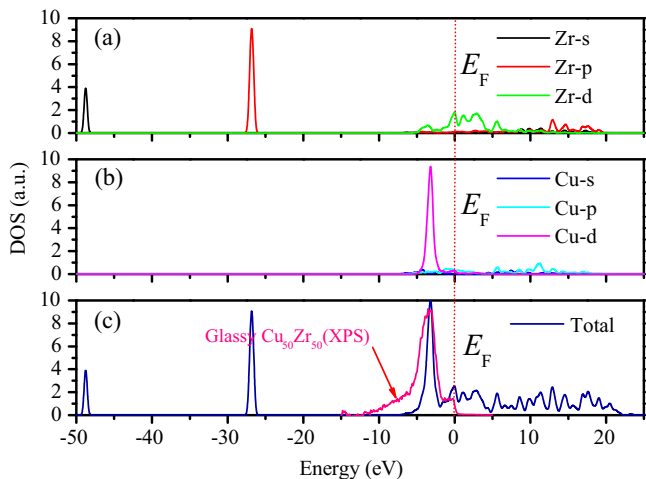
Fig. 4. Calculated DOS for Cu_1Zr_1 and measured DOS for $Cu_{50}Zr_{50}$ glass. (a) Partial DOS of Zr; (b) partial DOS of Cu; (c) comparing of the total DOS of $Cu_{50}Zr_{50}$ glass and the ordered compound Cu_1Zr_1.

below the curves is proportional to the total number of valence electrons (d, p, and s). This procedure was carried out after a background subtraction. Here, the value of DOS of $Cu_{50}Zr_{50}$ at Fermi level E_F is determined as 0.81 states/(eV atom), which is in excellent agreement with previous results [22]. The normalized total DOS of $Cu_{50}Zr_{50}$ from XPS and that of its crystalline counterpart Cu_1Zr_1 are compared in Fig. 4(c). Although the total DOS of $Cu_{50}Zr_{50}$ glass shows no sign of hyperfine structures, the center energy of the transition metal in the alloy lies in the energy range where the peak in the photoemission spectrum is observed. The results further illustrate that the value of DOS of $Cu_{50}Zr_{50}$ at Fermi level is mainly dominated by Zr.

In $Cu_{100-x}Zr_x$ glassy system, the electronic shells of Zr ($4d^2 5s^2$) and Cu ($3d^{10} 4s^1$) are different. The propensity of atoms in alloys to compete with other atomic species for valence-electron charge is generally encompassed in electronegativity factor [25,26]. The electronegativities of Cu and Zr are 1.88 and 1.37, respectively [27]. Thus, the electrons could transfer from the $4d$ of Zr atoms to fill the shells of Cu atoms, that is to say, the d energy bands of Zr is not filled in metallic state. The $4d$ shell is on the inside track, then the overlap of $4d$ energy bands of Zr is less and the bands are narrow in the process of metallic formation [19,28]. Therefore, there is a large value of DOS for $4d$ bands from Zr and it is essentially responsible for the value of DOS at Fermi level in $Cu_{100-x}Zr_x$ ($x = 40, 50, 60$) alloy system, similar to the fact that E and G values of MGs mainly inherit from the component Zr [13,15]. The results are helpful for understanding the inheritance of MGs and indicate that the elastic constants maybe related to the DOS at Fermi level. This work provides a new perspective on the structure–property relationship of MGs, which is helpful for designing new MGs with unique properties. However, there are still some critical issues need to be further explored, for example, the connection between the DOS at the Fermi level and elastic properties. To address these issues, more refined scrutiny of this connection will be desired in future work.

4. Conclusions

In this paper, the electronic DOS of $Cu_{100-x}Zr_x$ MGs was investigated by UPS, XPS and first-principles calculations. The results demonstrated that there is a large value of DOS for $4d$ bands from Zr and the values of DOS of $Cu_{100-x}Zr_x$ ($x = 40, 50, 60$) MGs at Fermi level E_F are always dominant by Zr rather than Cu. This work is helpful for understanding the inheritance of MGs and designing new MGs with unique properties.

References

[1] K.L. Edwards, E. Axinte, L.L. Tabacaru, A critical study of the emergence of glass and glassy metals as "green" materials, Mater. Des. 50 (2013) 713–723.
[2] Y. Huang, H. Fan, D. Wang, Y. Sun, F. Liu, J. Shen, et al., The effect of cooling rate on the wear performance of a ZrCuAlAg bulk metallic glass, Mater. Des. 58 (2014) 284–289.
[3] D.B. Miracle, A structural model for metallic glasses, Nat. Mater. 3 (2004) 697–702.
[4] A. Inoue, B. Shen, H. Koshiba, H. Kato, A.R. Yavari, Cobalt-based bulk glassy alloy with ultrahigh strength and soft magnetic properties, Nat. Mater. 2 (2003) 661–663.
[5] W. Yang, H. Liu, Y. Zhao, A. Inoue, K. Jiang, J. Huo, et al., Mechanical properties and structural features of novel Fe-based bulk metallic glasses with unprecedented plasticity, Sci. Rep. 4 (2014) 6233.
[6] K. Samwer, Hv. Löhneysen, Amorphous superconducting Zr_xCu_{1-x}: electronic properties, stability, and low-energy excitations, Phys. Rev. B 26 (1982) 107.
[7] C. Suryanarayana, A. Inoue, Iron-based bulk metallic glasses, Int. Mater. Rev. 58 (2013) 131–166.
[8] W.M. Yang, H.S. Liu, L. Xue, J.W. Li, C.C. Dun, J.H. Zhang, et al., Magnetic properties of $(Fe_{1-x}Ni_x)_{72}B_{20}Si_4Nb_4$ ($x = 0.0$–0.5) bulk metallic glasses, J. Magn. Magn. Mater. 335 (2013) 172–176.
[9] L. Xue, H. Liu, L. Dou, W. Yang, C. Chang, A. Inoue, et al., Soft magnetic properties and microstructure of $Fe_{84-x}Nb_2B_{14}Cu_x$ nanocrystalline alloys, Mater. Des. 56 (2014) 227–231.
[10] J. Lefebvre, M. Hilke, Z. Altounian, Superconductivity and short-range order in metallic glasses $Fe_xNi_{1-x}Zr_2$, Phys. Rev. B 79 (2009) 184525.
[11] E. Axinte, Metallic glasses from "alchemy" to pure science: present and future of design, processing and applications of glassy metals, Mater. Des. 35 (2012) 518–556.
[12] W. Zhao, G. Li, Y.Y. Wang, S.D. Feng, L. Qi, M.Z. Ma, et al., Atomic bond proportions and relations to physical properties in metallic glasses, Mater. Des. 65 (2015) 1048–1052.
[13] D. Ma, A.D. Stoica, X.L. Wang, Z.P. Lu, B. Clausen, D.W. Brown, Elastic moduli inheritance and the weakest link in bulk metallic glasses, Phys. Rev. Lett. 108 (2012) 085501.
[14] G. Li, Y. Wang, P. Liaw, Y. Li, R. Liu, Electronic structure inheritance and pressure-induced polyamorphism in lanthanide-based metallic glasses, Phys. Rev. Lett. 109 (2012) 125501.
[15] W.H. Wang, Properties inheritance in metallic glasses, J. Appl. Phys. 111 (2012) 123519.
[16] G.R. Garrett, M.D. Demetriou, J. Chen, W.L. Johnson, Effect of microalloying on the toughness of metallic glasses, Appl. Phys. Lett. 101 (2012) 241913.
[17] Q. Hu, M.W. Fu, X.R. Zeng, Thermostability and thermoplastic formability of $(Zr_{65}Cu_{17.5}Ni_{10}Al_{7.5})_{100-x}RE_x$ ($x = 0.25$–3.25, RE: Y, Gd, Tb, Dy, Ho, Er, Tm, Yb, Lu) bulk metallic glasses, Mater. Des. 64 (2014) 301–306.
[18] W. Yang, H. Liu, C. Dun, J. Li, Y. Zhao, B. Shen, Nearly free electron model to glass-forming ability of multi-component metallic glasses, J. Non-Cryst. Solids 361 (2013) 82–85.
[19] C. Kittel, Introduction to Solid State Physics, Chemical Industry Press, Beijing, 2005.
[20] M.G. Brik, I. Sildos, V. Kiisk, First-principles calculations of optical and electronic properties of pure and Sm3+-doped TiO2, Physica B 405 (2010) 2450–2456.
[21] J.G. Speight, Lang's Handbook of Chemistry, in: M. Graw-Hill (Ed.), London, 2005. p. 1.151.
[22] W. Ching, L. Song, S. Jaswal, Calculation of electron states in Cu_xZr_{1-x} glasses by the orthogonalized linear combination of atomic orbitals method, Phys. Rev. B 30 (1984) 544–552.
[23] P. Panissod, D. Guerra, A. Amamou, J. Durand, W. Johnson, W. Carter, et al., Local symmetry around the glass-former sites in amorphous metallic alloys through electric quadrupole effects, Phys. Rev. Lett. 44 (1980) 1465–1468.
[24] K. Tanaka, T. Saito, K. Suzuki, R. Hasegawa, Role of atomic bonding for compound and glass formation in Ni–Si, Pd–Si, and Ni–B systems, Phys. Rev. B 32 (1985) 6853–6860.

[25] D.V. Louzguine, A. Inoue, Electronegativity of the constituent rare-earth metals as a factor stabilizing the supercooled liquid region in Al-based metallic glasses, Appl. Phys. Lett. 79 (2001) 3410–3412.

[26] J. Zaanen, G. Sawatzky, J. Allen, Band gaps and electronic structure of transition-metal compounds, Phys. Rev. Lett. 55 (1985) 418.

[27] R. Watson, L. Bennett, Transition metals: d-hybridization, electronegativities, and structural stability of intermetallic compounds, Phys. Rev. B18 (1978) 6439–6449.

[28] P. Häussler, Interrelations between atomic and electronic structures-liquid and amorphous metals as model systems, Phys. Rep. 222 (1992) 65–143.